

Oxidation of Aniline to Nitrobenzene Catalysed by 1-Butyl-3-methyl imidazolium phosphotungstate Hybrid Material Using *m*-chloroperbenzoic Acid as an Oxidant

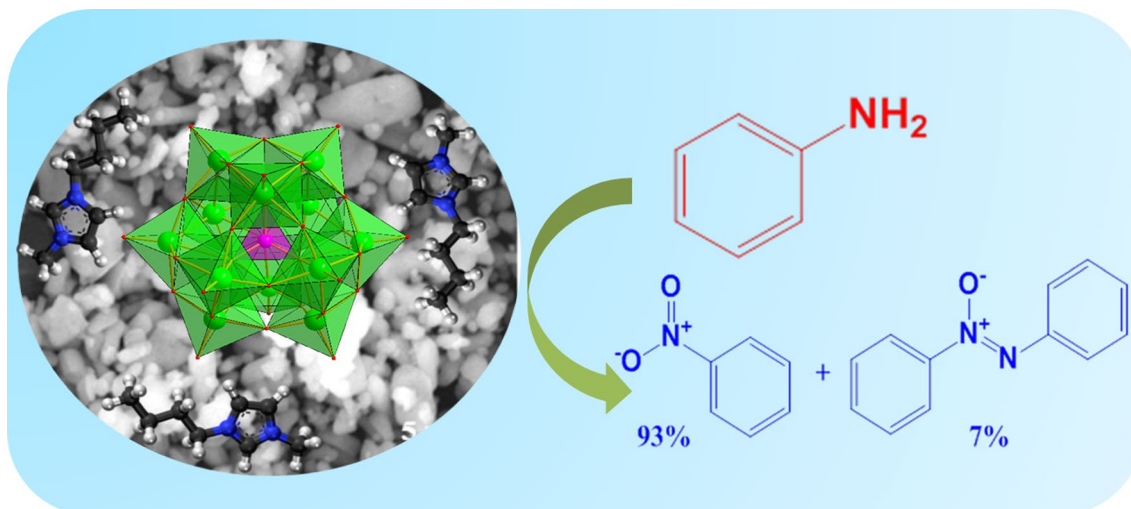
R. Meenakshi² · K. Shakeela¹ · S. Kutti Rani² · G. Ranga Rao¹

Received: 18 February 2017 / Accepted: 24 September 2017
© Springer Science+Business Media, LLC 2017

Abstract Keggin ion based hybrid materials, [BmIm]₃[PW₁₂O₄₀], [TBA]₃PW₁₂O₄₀ and [BuPy]₃PW₁₂O₄₀, were prepared by proton exchange with organic cations, 1-butyl-3-methyl imidazolium ion, tetrabutylammonium ion and butylpyridinium ion, respectively. The formation of hybrid materials was confirmed by FTIR, PXRD, SEM, TG-DTA, DSC analysis. These hybrid compounds are active

for oxidation of aniline using *m*-chloroperbenzoic acid as an oxidant. Among the three hybrid compounds, 1-butyl-3-methyl imidazolium phosphotungstate was found to be the best and efficient catalyst for selective aniline oxidation to nitrobenzene. It is a recoverable and reusable catalytic system. The redox property of the phosphotungstate cluster in the hybrid material is involved in the catalytic activity.

Graphical Abstract



✉ S. Kutti Rani
skrani@bsauniv.ac.in

✉ G. Ranga Rao
grrao@iitm.ac.in

¹ Department of Chemistry, Indian Institute of Technology Madras, Chennai, Tamil Nadu 600036, India

² Department of Chemistry, B.S. Abdur Rahman University, Vandalur, Chennai, Tamil Nadu 600048, India

Keywords Phosphotungstic acid · Ionic liquid · Hybrid material · Oxidation · Aniline

1 Introduction

Ionic liquids (ILs) are the salts which can melt below 100 °C, exclusively contain ionic species. They have been

used as catalysts, electrolytes and reaction media since they are thermally and electrochemically stable with no detectable vapour pressure, and high solvating power [1–5]. Keggin anions are one type of polyoxometalates (POMs) with general formula ($M=W, Mo$; $X=P, Si$) [6]. The structural diversities and wide variety of applications of polyoxometalates have been reviewed extensively [6–11]. They have been widely used as catalysts for organic transformations due to their controllable acidic and redox properties [11–17]. The combination of ionic liquids and POMs gives rise to hybrid materials in which the Keggin ions are fixed in the solid state. These hybrid molecular materials retain the properties of both the organic cations of ILs and inorganic anions of POMs [17–20].

The immobilized polyoxometalate hybrid materials have attracted attention in the area of heterogeneous catalysis [21–27]. Leng et al. reported the synthesis of heteropolyanion based ionic liquids as reaction induced self-separation catalysts for esterification of citric acid with *n*-butanol [21]. Series of Keggin type polyoxometalate-based ionic liquids have been used as efficient catalysts for deep desulfurization of fuels with H_2O_2 as oxidant [23]. The esterification of oleic acid for biodiesel production using $SiW_{12}O_{40}$ -based ionic liquid catalysts was reported by Zhen et al. [25]. In one of our earlier reports, silicotungstic acid has been immobilized onto the mesopores of amine-functionalized zirconia by electrostatic interactions. This hybrid is found to be an efficient heterogeneous catalyst for selective esterification of maleic acid with 98% conversion [26]. In another study, Yamaguchi et al. reported heterogeneous epoxidation of wide range of olefins with H_2O_2 using peroxotungstate immobilized on ionic liquid-modified SiO_2 [27].

The oxidation of aniline with various oxidants results in the formation of azoxybenzene, azobenzene, nitrosobenzene and nitrobenzene [28–32]. The product composition depends upon the reaction conditions and the nature of the catalyst employed, which need to be optimized to obtain nitrobenzene as a desired product. The selective oxidation of amines using polyoxometalates as catalysts has been reported earlier [32–36]. However, IL-POM hybrid materials are of current interest in organic transformations [12, 21]. We have prepared three IL-POM salts using ionic liquids containing 1-butyl-3-methyl imidazolium cation, tetrabutyl ammonium cation and butylpyridinium cation reacting with phosphotungstate Keggin anion (PWA) [18]. These IL-PWA hybrid materials are used as catalysts for selective oxidation of aniline to nitrobenzene reaction. We report that 1-butyl-3-methyl imidazolium phosphotungstate is more efficient catalyst for selective aniline oxidation using meta-chloroperoxybenzoic acid (*m*-CPBA) as an oxidant.

2 Experimental Section

2.1 Materials

1-bromobutane, 1-methyl imidazole and *m*-CPBA were purchased from Sigma-Aldrich. Phosphotungstic acid (PWA), tetrabutyl ammonium bromide (TBABr) were purchased from Loba Chemie and used as received. Pyridine, aniline and its substituted anilines were of analytical grade and used as received without purification. Purified solvents were used for all the catalytic reactions.

2.2 Materials Synthesis

The catalyst 1-butyl-3-methylimidazolium phosphotungstate hybrid material $[BmIm]_3[PW_{12}O_{40}]$ was synthesized as reported in literature [18]. 1-bromobutane was added to 1-methyl imidazole in a equimolar ratio of 0.24 mol and stirred at 80 °C for 24 h. The yellowish ionic liquid 1-butyl 3-methyl imidazolium bromide (BMImBr) was obtained in the lower phase. The unreacted starting material in the upper phase was removed by washing with ethyl acetate. *N*-butyl pyridinium bromide (BuPyBr) was prepared in a similar manner according to reported procedure [37]. We have chosen the ionic liquids which contain the cations, BMIm⁺, TBA⁺, and BuPy⁺. Each of these cations is reacted with $H_3PW_{12}O_{40} \cdot nH_2O$ in 3:1 mol ratio to obtain one mole of hybrid material, IL-POM. Typically, BMImBr (0.013 mol) was added drop wise to the solution containing (0.0048 mol) of phosphotungstic acid under constant stirring at room temperature. The white precipitate obtained was washed with distilled water and dried at 80 °C overnight. $[TBA]_3PW_{12}O_{40}$ and $[BuPy]_3PW_{12}O_{40}$ were also synthesized in a similar manner using TBABr and BuPyBr. The scheme of preparation of IL-POM hybrid catalysts is given Scheme 1.

2.3 Characterization

The FTIR spectra of the samples were recorded using JASCO FT/IR-6300 in the range of 4000–400 cm^{-1} . The XRD pattern of the materials were obtained using Bruker AXS D8 advanced powder XRD with CuK_{α} ($\lambda = 1.5406 \text{ \AA}$) radiation at settings of 40 kV and 30 mA with a divergence of 0.982. The thermal stability was recorded on TGA (Perkin-Elmer) Q500 V20.10 high resolution Thermogravimetric Analyzer in nitrogen atmosphere (flow rate = 20 ml/min) in the temperature range of 30–1000 °C at a heating rate of 5 °C/min. The phase transition of the materials was tested on a DSC (Perkin-Elmer) Q200 MDSC V24.4 of build 116. The surface morphology and elemental composition of

the materials were recorded using an FEI QUANTA 200F microscope. ^{31}P NMR spectra of fresh and reused catalysts in DMSO-d_6 solvent were recorded on a Bruker-FT-NMR-400 MHz spectrometer. The products formed in the aniline conversion reaction were analysed by gas chromatograph (Shimadzu 2014) employing capillary column (Rtx-5, $30\text{ m} \times 0.32\text{ mm}$, ID $1\text{ }\mu\text{m}$) and flame ionisation detector and further confirmed by gas chromatography-mass spectrometry (Perkin Elmer). The Clarus 680 chromatograph with capillary column (Elite-5MS, $30\text{ m} \times 0.25\text{ mm}$ ID $\times 250\text{ }\mu\text{m}$ df) was connected with Clarus 600 (EI) mass spectrometer.

2.4 Catalytic Oxidation of Aniline

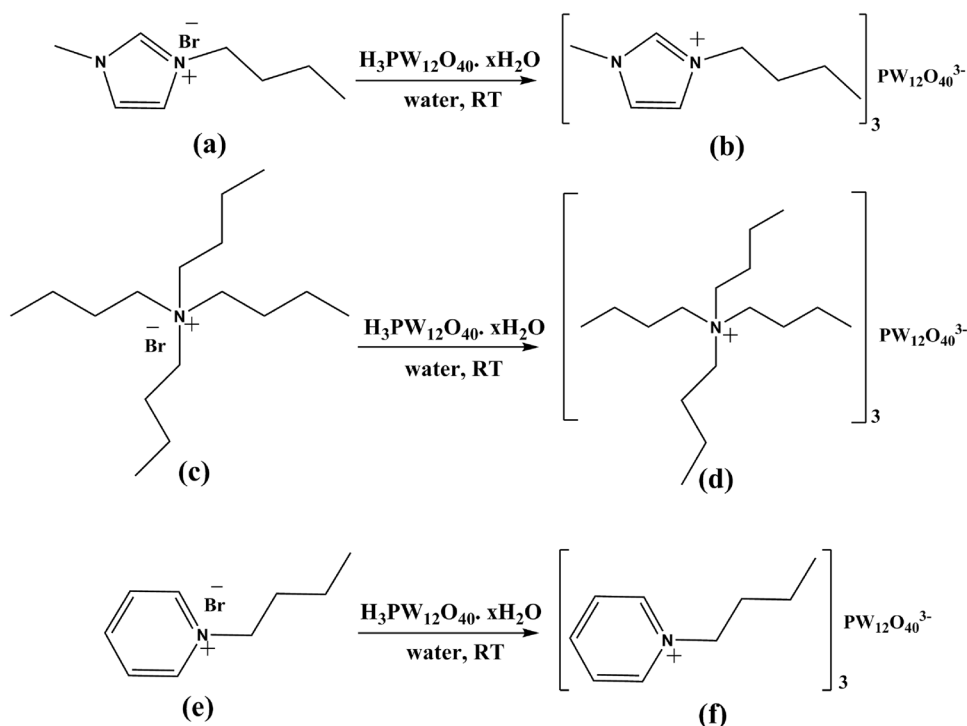
The oxidation of aniline using 1-butyl-3-methyl imidazolium phosphotungstate and *m*-CPBA was investigated.

m-chloroperbenzoic acid is a stronger oxidizing agent with outstanding reactivity and greater selectivity when compared to hydrogen peroxide and other per acids [38]. The addition of 2.67 mmol of *m*-CPBA to a stirred solution containing 0.053 mmol of the catalyst and 0.53 mmol of aniline in 3 ml of acetonitrile resulted in green coloured solution which indicates the formation of nitrosobenzene intermediate. The reaction mixture was stirred at $85\text{ }^\circ\text{C}$ for 2 h. Diethyl ether was added to the reaction mixture to re-precipitate the catalyst and recover it by filtration. The ether layer was washed with saturated bicarbonate solution to remove the *m*-chlorobenzoic acid byproduct. The final product was recovered by evaporating ether and analyzed by gas chromatograph and FID detector. The formation of the products were further confirmed by gas chromatography-mass spectrometry. The conversion of aniline and product selectivity were calculated by using the expressions,

$$\text{Conversion (mol \%)} = \frac{\text{Initial mol \% of aniline} - \text{Final mol \% of aniline}}{\text{Initial mol \% of aniline}} \times 100$$

$$\text{Selectivity of nitrobenzene (\%)} = \frac{\text{GC peak area of nitrobenzene}}{\text{Sum of GC peak areas of azoxybenzene and nitrobenzene}} \times 100$$

Scheme 1 Synthesis of different cation substituted phosphotungstates. **a** BMImBr, **b** [BMIm] $_3$ PW $_{12}$ O $_{40}$, **c** TBABr, **d** [TBA] $_3$ PW $_{12}$ O $_{40}$, **e** BuPyBr and **f** [BuPy] $_3$ PW $_{12}$ O $_{40}$



3 Results and Discussion

3.1 Physicochemical Characterization

The FTIR spectra of the prepared catalysts and their precursors are shown in Fig. 1. The inorganic moiety and phosphotungstate anion show four noticeable stretching vibrations in the region of 700–1100 cm^{-1} [39]. The P–O stretching of all the hybrids observed at 1079 cm^{-1} is analogous to that of the parent phosphotungstate anion. $\text{W}=\text{O}_{\text{terminal}}$ stretching is shifted from 985 to 974 cm^{-1} and the $\text{W}-\text{O}_e-\text{W}$ vibration also marginally blue shifted. Hence, the primary Keggin structure has been well retained in all the catalysts. The peak at 620 cm^{-1} corresponds to $\text{C}_2-\text{N}_1-\text{C}_5$ bending related to $[\text{BmIm}]_3\text{PW}_{12}\text{O}_{40}$ is analogous to that observed in the parent ionic liquid BmImBr [18]. The Im^+ ring stretching vibration observed at 1569 cm^{-1} for the ionic liquid shifted to 1564 cm^{-1} in the hybrid material. The Im^+ ring C–H stretch of the hybrid material is shifted to 2947 and 3128 cm^{-1} [18]. All the hybrids, $[\text{BmIm}]_3\text{PW}_{12}\text{O}_{40}$, $[\text{TBA}]_3\text{PW}_{12}\text{O}_{40}$, $[\text{BuPy}]_3\text{PW}_{12}\text{O}_{40}$ revealed peak shifts in the region 2800–3000 cm^{-1} which are attributed to butyl C–H stretching vibrations. The two hybrid materials, except $[\text{TBA}]_3\text{PW}_{12}\text{O}_{40}$, show vibrational bands characteristic of aromatic C=C bonds. The heterocyclic C–H stretching and bending of BuPyBr are observed at 2957 and 1175 cm^{-1} . For $[\text{BuPy}]_3\text{PW}_{12}\text{O}_{40}$ hybrid material, these frequencies are shifted to 2953 and 1167 cm^{-1} respectively. The bending vibration of Ar–H observed at 682 cm^{-1} is analogous to that of BuPyBr .

Figure 2 shows the powder XRD pattern of the three hybrid materials. Phosphotungstic acid shows the characteristic high intensity peak at 10.29° (JCPDS No: 752125). The hybrid material, however, shows new intense peaks in the low angle region while the intensity of the peaks in the high angle region decreased [40]. The three acidic protons and most of the H_2O molecules of phosphotungstic acid are replaced by three molecules of organic cations (BmIm^+ , TBA^+ , BuPy^+). The intense peaks in the low angle region in Fig. 2 indicate the formation of well-defined layered-type structures in all the three compounds. For $[\text{BmIm}]_3\text{PW}_{12}\text{O}_{40}$, the diffraction pattern shows four distinct peaks with an intense peak at $2\theta = 8.7$ corresponding to the d-spacing of 1.0 nm. The d-spacing value agreed with the theoretical size of the IL–POM hybrids [41]. Similar pattern has been observed for $[\text{BuPy}]_3\text{PW}_{12}\text{O}_{40}$ with little shift in the 2θ values. The d-spacing value analogous to the high intense peak ($2\theta = 8.8$) is 0.99 nm. In contrast to other two catalysts, the XRD pattern of $[\text{TBA}]_3\text{PW}_{12}\text{O}_{40}$ exhibits peaks merged with high intensity peak at $2\theta = 8.0$ with d-spacing value of 1.1 nm. The combined peaks indicated the presence of closely packed crystal structures relating to the large number

of bulky tetra butyl ammonium ions around phosphotungstate anions [18, 40].

The thermal behaviour of all the catalysts under nitrogen atmosphere has been studied by TGA and DSC as shown in the Figs. 3 and 4, respectively. The results are tabulated in Table 1. From Fig. 3, it is observed that all the catalysts showed dual weight losses corresponding to the organic cation followed by inorganic Keggin anion. The pure phosphotungstic acid generally decomposes at 550 °C leading to WO_3 and P_2O_5 residues. From Table 1, it could be seen that the thermal stability (T_{onset}) and maximum degradation (T_{max}) followed the trend $[\text{TBA}]_3 < [\text{BuPy}]_3 < [\text{BmIm}]_3$. The high stability of $[\text{BmIm}]_3\text{PW}_{12}\text{O}_{40}$ indicated the stronger interaction between imidazolium cation and phosphotungstate anion, primarily due to better delocalisation of positive charge than pyridinium and ammonium cations [40, 42]. The TGA curve of $[\text{TBA}]_3\text{PW}_{12}\text{O}_{40}$ in Fig. 3b shows a steep fall (19% weight loss) in the region 330–460 °C, resulting from the decomposition of organic moiety possessing greater number of butyl groups around Keggin anion, when compared to $[\text{BmIm}]_3\text{PW}_{12}\text{O}_{40}$ (9% weight loss, Fig. 3a) and $[\text{BuPy}]_3\text{PW}_{12}\text{O}_{40}$ (7% weight loss, Fig. 3c).

The endothermic peak of DSC curves (Fig. 4; Table 1) at 189, 206 and 238 °C demonstrate the solid to liquid transition of $[\text{BmIm}]_3\text{PW}_{12}\text{O}_{40}$, $[\text{TBA}]_3\text{PW}_{12}\text{O}_{40}$ and $[\text{BuPy}]_3\text{PW}_{12}\text{O}_{40}$ respectively. T_m followed the trend $[\text{BmIm}]_3 < [\text{TBA}]_3 < [\text{BuPy}]_3$. Generally, melting point will be high when packing of molecules is even and ordered. $[\text{BuPy}]_3\text{PW}_{12}\text{O}_{40}$ is planar and symmetric. Hence its melting point is higher than $[\text{BmIm}]_3\text{PW}_{12}\text{O}_{40}$ and $[\text{TBA}]_3\text{PW}_{12}\text{O}_{40}$. The peak observed at 169 °C for $[\text{BmIm}]_3\text{PW}_{12}\text{O}_{40}$ corresponds to the presence of an eutectic impurity in the sample. Elemental analysis revealed the presence of two water molecules in the $[\text{BmIm}]_3\text{PW}_{12}\text{O}_{40}$ hybrid (Calculated C-8.5, H-1.48, N-1.52, and Experimental C-8.73, H-1.50, N-2.35). Hence, the eutectic impurity is expected to be due to weak hydrogen bonding in $[\text{BmIm}]_3\text{PW}_{12}\text{O}_{40}$ hybrid.

The surface morphologies of the three powder materials are shown in Fig. 5. Capsule like particles with smooth surfaces are observed for $[\text{BmIm}]_3\text{PW}_{12}\text{O}_{40}$ and $[\text{BuPy}]_3\text{PW}_{12}\text{O}_{40}$ due to the regular arrangement of three butyl groups around the phosphotungstate ions. However, granular like particles are observed for $[\text{TBA}]_3\text{PW}_{12}\text{O}_{40}$ which might be due to the random arrangement of large number of butyl groups around the phosphotungstate ion. This can be correlated with the presence of merged diffraction peaks observed in PXRD of $[\text{TBA}]_3\text{PW}_{12}\text{O}_{40}$.

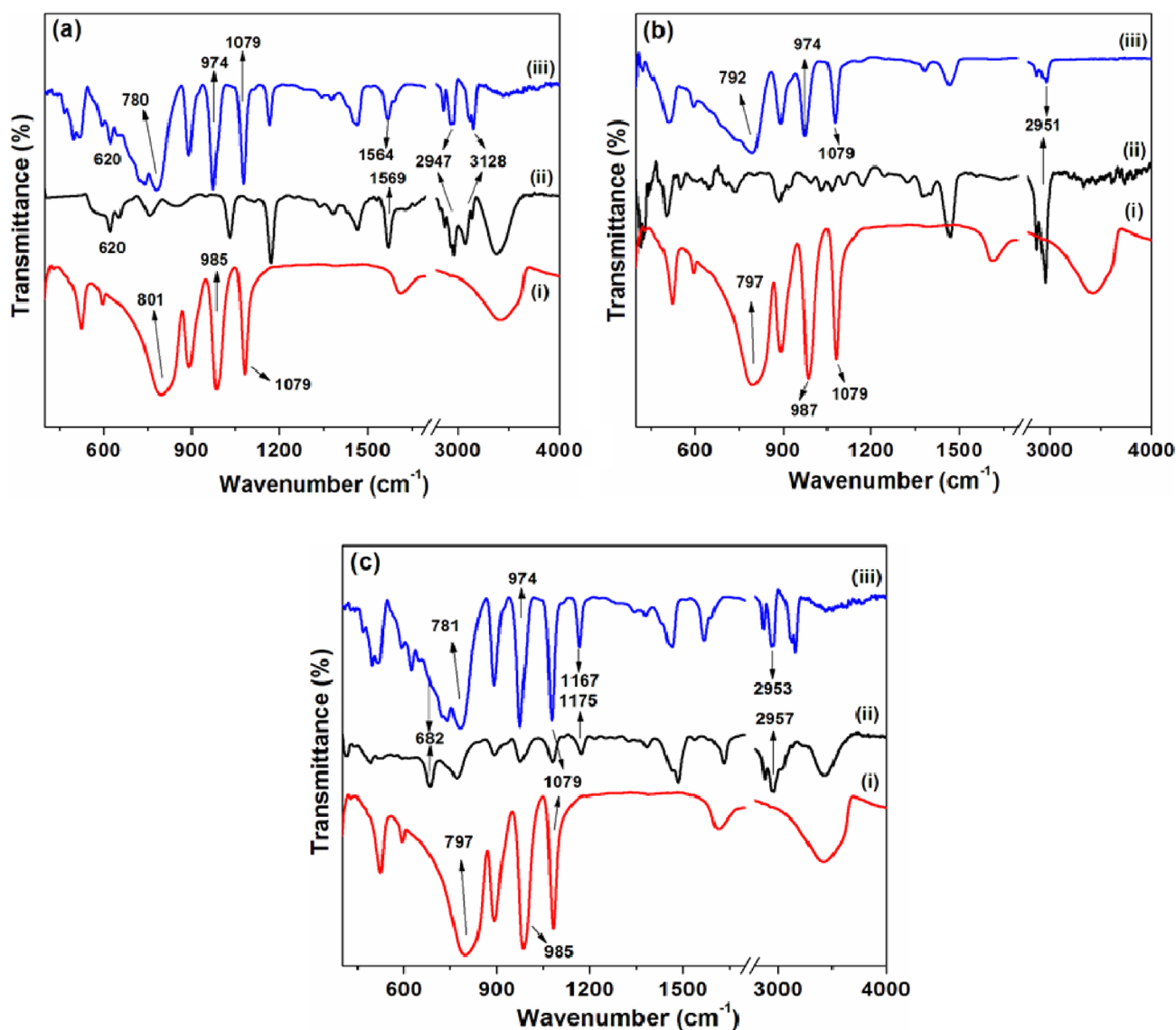


Fig. 1 FTIR spectrum of **a** (i) $\text{H}_3\text{PW}_{12}\text{O}_{40}$, (ii) BMIImBr, (iii) $[\text{BMIIm}]_3\text{PW}_{12}\text{O}_{40}$, **b** (i) $\text{H}_3\text{PW}_{12}\text{O}_{40}$, (ii) [TBA]Br, (iii) $[\text{TBA}]_3\text{PW}_{12}\text{O}_{40}$, **c** (i) $\text{H}_3\text{PW}_{12}\text{O}_{40}$, (ii) [BuPy]Br, (iii) $[\text{BuPy}]_3\text{PW}_{12}\text{O}_{40}$

3.2 Aniline Oxidation Reaction

3.2.1 Influence of Reaction Conditions

The oxidation of aniline gives variety of products as depicted in Scheme 2. The reaction parameters like solvents, temperature, concentration of aniline and meta-chloro-perbenzoic acid (*m*-CPBA) are optimized for $[\text{BmIm}]_3\text{PW}_{12}\text{O}_{40}$ catalyst. The effect of solvents on the oxidation of aniline over $[\text{BMIIm}]_3\text{PW}_{12}\text{O}_{40}$ catalyst at 85 °C is given in Table 2. The compound $[\text{BMIIm}]_3\text{PW}_{12}\text{O}_{40}$ dissolves in acetonitrile and acts as a homogeneous catalyst while in other solvents it acts as solid–liquid heterogeneous catalyst. High conversion (> 90%) of aniline in all the solvents was observed, but the

conversion is 100% in acetonitrile with greater selectivity (93%) to nitrobenzene. Under homogeneous conditions, the nitroso intermediate would be better stabilised by the imidazolium groups in the catalyst which on further oxidation gives nitro product [43].

Under homogeneous condition, variation of reaction parameters like amount of oxidant, substrate, catalyst and the temperature on aniline oxidation was studied as shown in Fig. 6. The equimolar concentration of substrate and oxidant (0.53 mmol) at 85 °C resulted in moderate conversion of aniline (67%). As seen in Fig. 6a, the formation of insignificant amount of azobenzene (not shown) and azoxybenzene is favoured initially due to the insufficient amount of oxidant. The oxidative coupling of nitrosobenzene intermediate

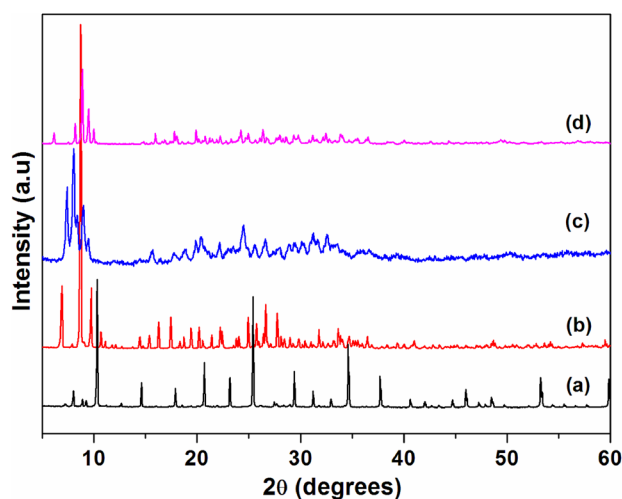


Fig. 2 XRD pattern of (a) H₃PW₁₂O₄₀, (b) [BMIm]₃PW₁₂O₄₀, (c) [TBA]₃PW₁₂O₄₀, (d) [BuPy]₃PW₁₂O₄₀

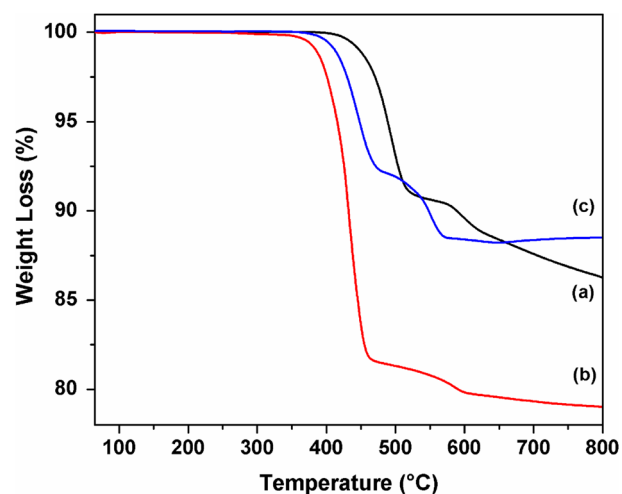


Fig. 3 TGA pattern of (a) [BMIm]₃PW₁₂O₄₀, (b) [TBA]₃PW₁₂O₄₀, (c) [BuPy]₃PW₁₂O₄₀

formed might have reacted primarily with unreacted aniline or phenyl hydroxylamine resulting in the formation of azoxybenzene, which can convert to azobenzene as shown in Scheme 2. At this point, the doubling the catalyst concentration resulted in 86% conversion with 54 and 44% selectivity for azoxy and azobenzene, respectively. Further increase in the concentration of oxidant with 0.053 mmol of catalyst resulted in complete conversion of aniline with high selectivity towards nitrobenzene (Fig. 6a). The use of 2.67 mmol of oxidant predominantly favoured the formation of the selective product nitrobenzene (96% GC yield). With 2.67 mmol of oxidant, in the absence of catalyst, oxidation after two hours at 85 °C resulted in a mixture of products with 48, 35, and 10% of azoxy, nitroso and nitrobenzene, respectively.

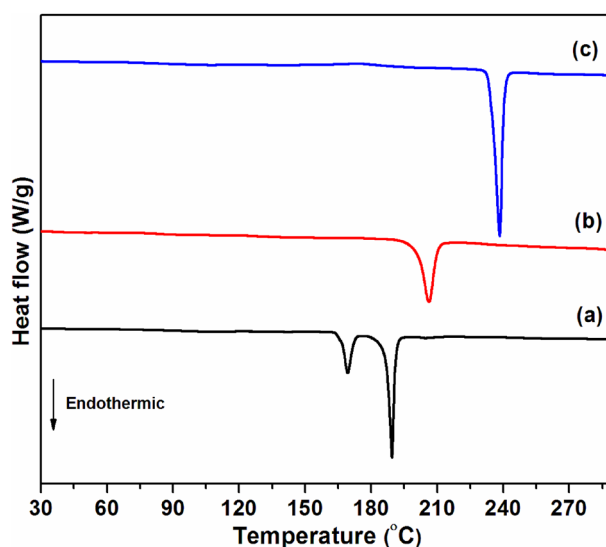


Fig. 4 DSC pattern of (a) [BMIm]₃PW₁₂O₄₀, (b) [TBA]₃PW₁₂O₄₀, (c) [BuPy]₃PW₁₂O₄₀

Table 1 Thermal properties of various cation substituted phosphotungstates

Catalyst	T _{onset} (°C)	T _{max} (°C)	Residue (%)	T _m (°C)
[BmIm] ₃ [PW ₁₂ O ₄₀]	378	493	85	189
(TBA) ₃ PW ₁₂ O ₄₀	336	432	78	206
(BuPy) ₃ PW ₁₂ O ₄₀	355	446	88	238

Also, the oxidation of aniline in acetonitrile using *m*-CPBA as oxidant, in the absence of catalyst, for 10 h resulted in lower yield of nitrobenzene, as reported by Liu et al. [44]. This emphasizes the importance of the hybrid catalyst in the oxidation of aniline. Increasing catalyst concentration up to 0.053 mmol resulted in high selectivity to nitrobenzene (Fig. 6b). The imidazolium groups in the catalyst would stabilise the nitroso intermediate under homogeneous conditions, which on further oxidation resulted in the nitro product [43]. At higher catalyst concentrations, there is a possibility of parallel oxidative coupling between nitroso with phenyl hydroxylamine, thereby leading to slight decrease in nitro selectivity (78%). Low substrate concentrations result in nitrobenzene as a major product (Fig. 6c). The substrate concentration above 1 mmol favours the formation of nitrosobenzene intermediate. The nitrosobenzene intermediate might have reacted with phenylhydroxylamine to form azoxybenzene which would have been converted to azobenzene for further increase in substrate concentration. Figure 6d shows the enhanced selectivity towards nitrobenzene with increase in temperature [33]. Nitrosobenzene intermediate was not observed at the temperatures studied. The optimized reaction conditions for obtaining nitrobenzene

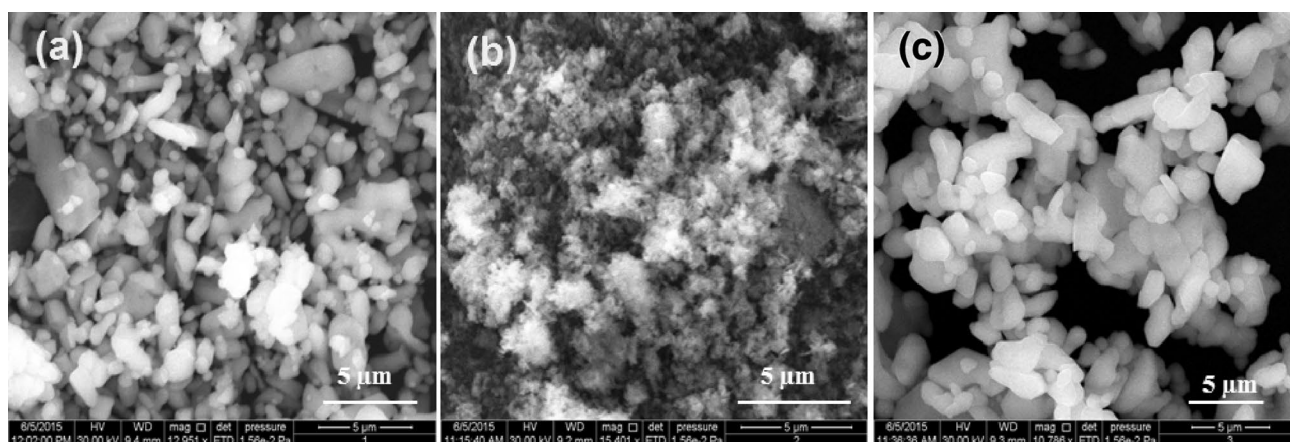
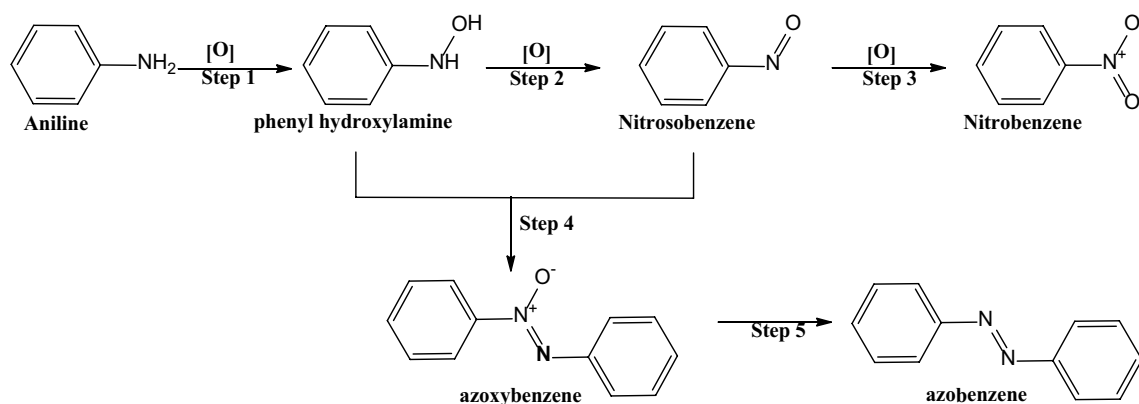


Fig. 5 SEM images of **a** [BmIm]₃PW₁₂O₄₀, **b** [TBA]₃PW₁₂O₄₀, and **c** [BuPy]₃PW₁₂O₄₀



Scheme 2 Products of aniline oxidation

Table 2 Influence of various solvents on aniline oxidation using [BmIm]₃PW₁₂O₄₀ catalyst^a

Sl. No.	Solvent	Solubility	Conversion ^b (%)	Selectivity ^c (%)
1	Ethyl acetate	Insoluble	100	45
2	Toluene	Insoluble	92	75
3	Ethanol	Insoluble	92	70
4	Acetonitrile	Soluble	100	93

^aAniline (0.53 mmol), *m*-CPBA (2.67 mmol), catalyst (0.053 mmol), 85 °C, 2 h

^bConversion of aniline

^cSelectivity for nitrobenzene

selectively are 0.53 mmol of substrate, 2.67 mmol of *m*-CPBA, 0.053 mmol of [BmIm]₃PW₁₂O₄₀ catalyst and 85 °C in 2 h.

The product distribution of aniline oxidation using cation substituted phosphotungstates as catalysts and *m*-CPBA

as oxidant are summarized in Table 3. The selectivity for nitrobenzene is only 10% in the absence of the catalyst. The homogeneous Keggin structure H₃PW₁₂O₄₀ resulted in 100% conversion with 83% selectivity to nitrobenzene. Though this catalyst gives better selectivity towards nitrobenzene, the complete recovery of the catalyst is difficult. The oxidation of aniline catalyzed by Na₁₂[WZnZn₂(H₂O)₂(ZnW₉O₃₄)₂] in aqueous biphasic reaction medium resulted in azoxybenzene as the major product [33]. Tetranuclear peroxotungstate TPA₃[H{W₂O₂(O₂)₄(μ-O)}₂] resulted in nitrosobenzene as 85% selective product in the presence of H₂O₂ oxidant [34]. Various other polyoxometalate catalysts have shown much less selectivities compared to [BmIm]₃PW₁₂O₄₀ and [TBA]₃PW₁₂O₄₀ IL-POM hybrid catalysts. Even though the aniline oxidation by [BmIm]₃PW₁₂O₄₀ catalyst is homogeneous, the recovery of the catalyst can be done by precipitation method using low polar solvent like diethyl ether. However, recovery of [TBA]₃PW₁₂O₄₀ catalyst is not possible because the tetra butyl groups seem to enhance partial solubility of [TBA]₃PW₁₂O₄₀ in ether. The hybrid catalyst

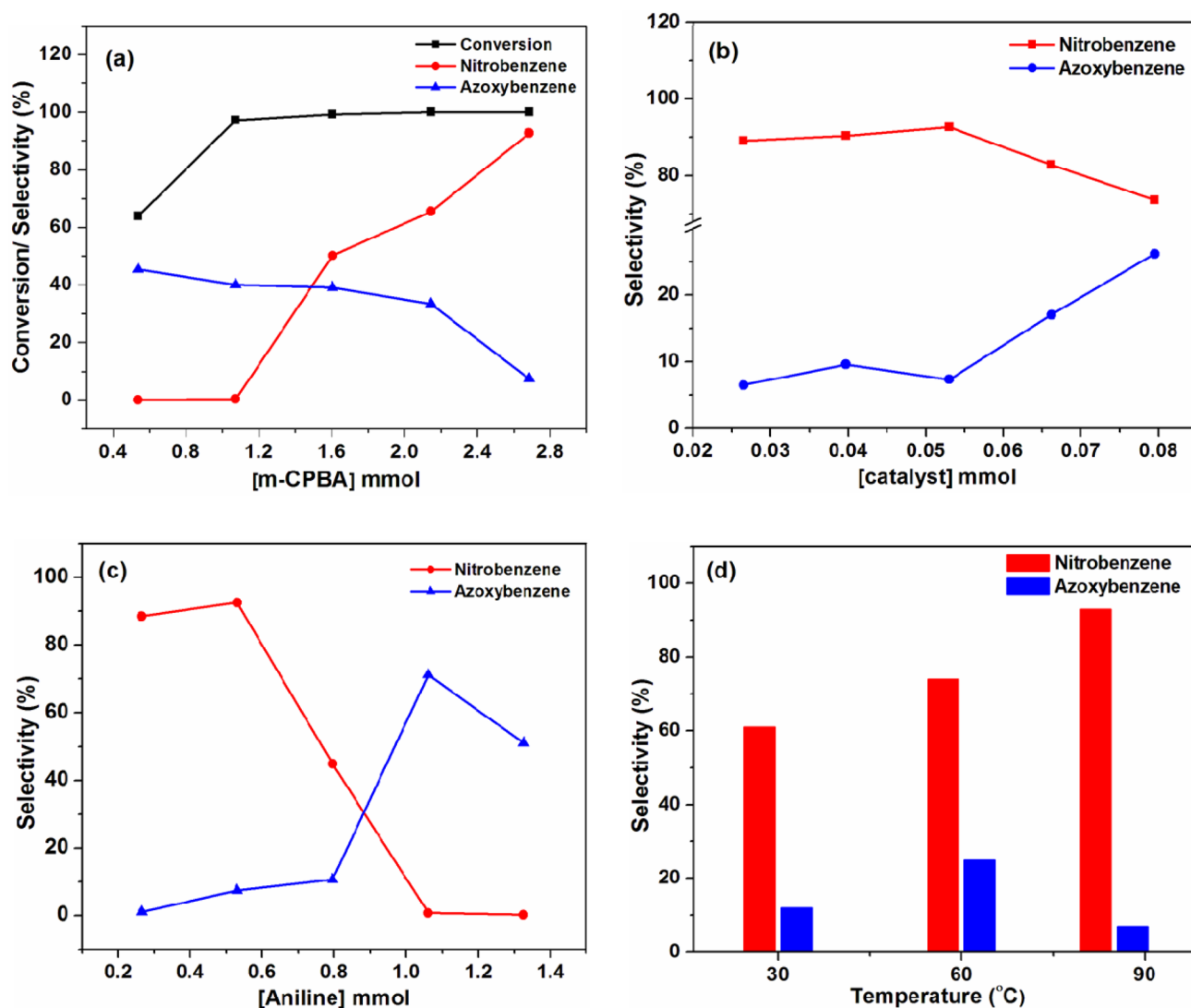


Fig. 6 Effect of reaction parameters on the oxidation of aniline using *m*-CPBA oxidant over [BmIm]₃PW₁₂O₄₀ catalyst: **a** oxidant concentration, **b** catalyst concentration, **c** substrate concentration and **d** reaction temperature

[BuPy]₃PW₁₂O₄₀ shows good conversion under heterogeneous conditions but the selectivity towards nitrobenzene is very less due to poor stabilization of nitroso intermediate by the catalyst.

The efficiency of *m*-CPBA is compared with peroxo oxidants like H₂O₂ and tetrabutyl hydrogen peroxide (TBHP) under optimised reaction conditions using [BmIm]₃[PW₁₂O₄₀] catalyst (Table 4). The conversion of aniline is 66% with H₂O₂ as an oxidant resulting in nitrobenzene as a minor product. The use of H₂O₂ as oxidant generally results in product nitrosobenzene [32, 34], azoxybenzene [33, 35] and azobenzene [45]. Aniline reacting with H₂O₂ in CHCl₃, in the presence of peroxotungstophosphate as heterogeneous catalyst, does not produce nitrobenzene at room temperature [32]. There have been no reports in the literature regarding the use of POM and IL-POM hybrids

as catalysts for aniline oxidation with TBHP and *m*-CPBA as oxidants. About 77% of unreacted aniline was observed when TBHP was used as an oxidant (Entry 3, Table 4). Under the optimised reaction conditions, no selective product was observed using H₂O₂ and TBHP as oxidants. Hence, only *m*-CPBA is the best oxidant to obtain nitrobenzene with highest selectivity (Entry 1, Table 4).

The plausible reaction mechanism of the oxidation of aniline by *m*-chloroperbenzoic acid as oxidant is given in Scheme 3. The phosphotungstate moiety in the hybrid [BmIm]₃[PW₁₂O₄₀] reacts with *m*-CPBA to generate peroxo-species {PO₄[WO(O₂)₂]₄}³⁻, which can act as active oxygen transfer agent [46]. This further reacts with aniline to produce nitrobenzene, as depicted in Scheme 3.

In order to evaluate the ease of the oxidation process, the reaction is carried out using different substituted aniline

Table 3 Oxidation of aniline catalysed by various polyoxometalates with *m*-CPBA^a

Sl. No.	Catalyst	Oxidant	Reaction medium	Product selectivity	Selectivity %	References
1	No catalyst	<i>m</i> -CPBA	Homo	Nitro	10	Present work
2	H ₃ PW ₁₂ O ₄₀	<i>m</i> -CPBA	Homo	Nitro	83	Present work
3	Na ₁₂ [WZnZn ₂ (H ₂ O) ₂ (ZnW ₉ O ₃₄) ₂] ^b	H ₂ O ₂	Homo	Azoxy	95	[33]
4	TPA ₃ [H{W ₂ O ₂ (O ₂) ₄ (μ-O)} ₂] ^c	H ₂ O ₂	Homo	Nitroso	85	[34]
5	[PyN ⁺ (CH ₂) ₁₅ CH ₃] ₃ (PO ₄ [W(O)(O ₂) ₂] ₄) ^{3-d}	H ₂ O ₂	Homo	Nitro	13	[32]
6	[PyN ⁺ (CH ₂) ₁₅ CH ₃] ₃ (PO ₄ [W(O)(O ₂) ₂] ₄) ^{3-e}	H ₂ O ₂	Homo	Nitro	71	[32]
7	[BmIm] ₃ PW ₁₂ O ₄₀ ^f	<i>m</i> -CPBA	Homo	Nitro	62	Present Work
8	[BmIm] ₃ PW ₁₂ O ₄₀	<i>m</i> -CPBA	Homo	Nitro	93	Present work
9	[TBA] ₃ PW ₁₂ O ₄₀	<i>m</i> -CPBA	Homo	Nitro	90	Present work
10	[BuPy] ₃ PW ₁₂ O ₄₀	<i>m</i> -CPBA	Hetero	Nitro	4	Present work

Reaction conditions:

^aAniline (0.53 mmol), *m*-CPBA (2.67 mmol), acetonitrile (3 ml), 85 °C, 2 h

^bAniline (1 mmol), H₂O₂ (5 mmol), water (1 ml), 75 °C, 7 h

^cAniline (1 mmol), H₂O₂ (2 mmol) catalyst (5 μmol)

^dAniline (3 mmol), H₂O₂ (9 mmol), chloroform (7.5 ml), RT, 2 h

^eAniline (3 mmol), H₂O₂ (9 mmol), chloroform (7.5 ml), reflux, 4 h

^fAniline (0.53 mmol), *m*-CPBA (2.67 mmol), acetonitrile (3 ml), RT, 2 h

substrates under the same optimized reaction conditions (Table 5). Firouzabadi et al. reported the conversion of anilines substituted with electron-donating groups selectively to

Table 4 Effect of various oxidants on aniline oxidation using [BmIm]₃[PW₁₂O₄₀] catalyst^a

Entry	Oxidant	Conversion ^b (%)	% Nitrobenzene ^c (selectivity)
1	<i>m</i> -CPBA	100	93
2	H ₂ O ₂	66	10
3	TBHP	23	<1

^aAniline (0.53 mmol), catalyst (0.053 mmol), acetonitrile (3 ml), 85 °C, 2 h

^bConversion of aniline

^cSelectivity for nitrobenzene

the corresponding nitro compounds with sodium perborate in the presence of tungstophosphoric acid and surfactants [35]. Though nitrobenzene is obtained as the selective product, catalyst recovery is not possible. The use of excess sodium perborate (NaBO₃) in acetic acid for the oxidation of anilines containing electron-withdrawing groups to the corresponding nitro compounds has been reported by McKillop [47]. But anilines with electron-donating groups are oxidized to the nitro compounds in very low yields [48]. Hence this method appears inappropriate for this type of oxidation reactions. Under optimized conditions, we have observed that the substituents with both electron withdrawing and donating groups irrespective of their positions (ortho, meta and para) resulted in corresponding nitro derivatives with high selectivity, which is in contrast to the reported procedures [35, 47, 48]. The products obtained by the oxidation of aniline derivatives have been confirmed using gas chromatography-mass spectrometry.

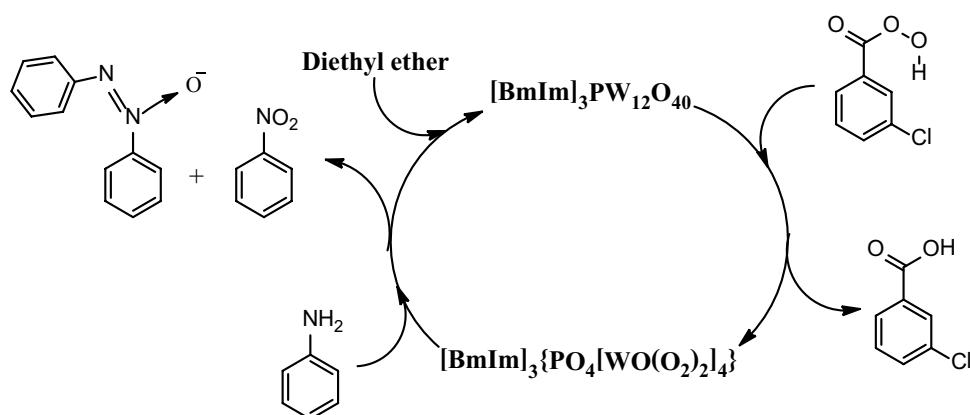
Scheme 3 Mechanism of aniline oxidation catalysed by [BmIm]₃[PW₁₂O₄₀]

Table 5 Oxidation of derivatives of aniline using $[\text{BmIm}]_3[\text{PW}_{12}\text{O}_{40}]$ as catalyst^a

Sl. No.	Substrate	Product	%Nitrobenzene (selectivity)
1			98
2			100
3			96
4			92
5			98
6			98
7			100
8			98
9			87

^a m -CPBA : 2.67 mmol, Catalyst: 0.053 mmol, acetonitrile: 3 ml, 85 °C, 2 h

3.2.2 Reusability Test

Though $[\text{BmIm}]_3\text{PW}_{12}\text{O}_{40}$ is soluble in acetonitrile, it is reprecipitated with diethyl ether and then recovered by filtration for reuse. Nearly 100% conversion of aniline has been observed in all the four runs indicating the steady reusability of the catalyst. But the selectivity to nitrobenzene decreased from 92% in the first run to 83% in the fourth run. Hence, it could be established that the catalyst could be reused thrice without much loss of catalytic activity, as shown in Fig. 7. The IR spectrum of the reused catalyst is similar to that of fresh catalyst with reduced intensity (Fig. 8). Though the

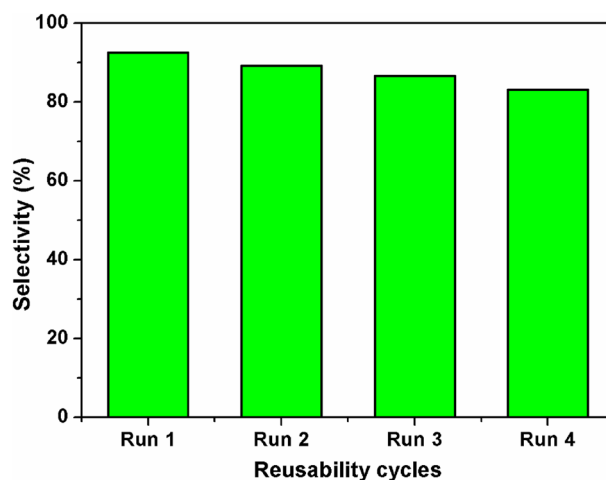


Fig. 7 Reusability of $[\text{BmIm}]_3\text{PW}_{12}\text{O}_{40}$, reaction conditions: m -CPBA: 2.67 mmol, Catalyst: 0.053 mmol, acetonitrile: 3 ml, 85 °C, 2 h

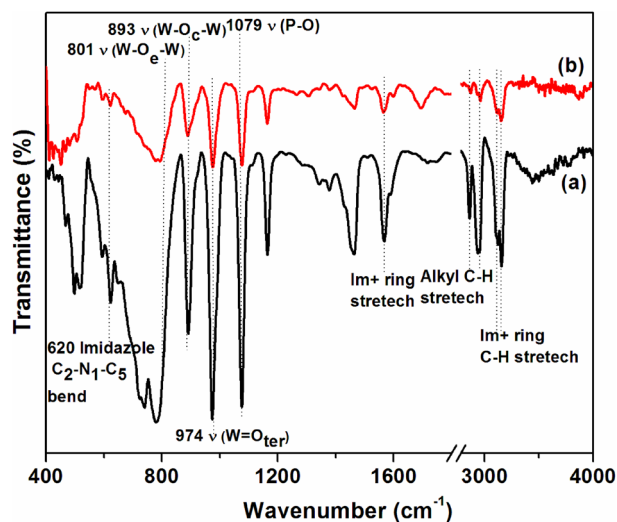


Fig. 8 FTIR spectrum of 1-butyl-3-methyl imidazolium phosphotungstate catalyst (a) fresh and (b) four times reused

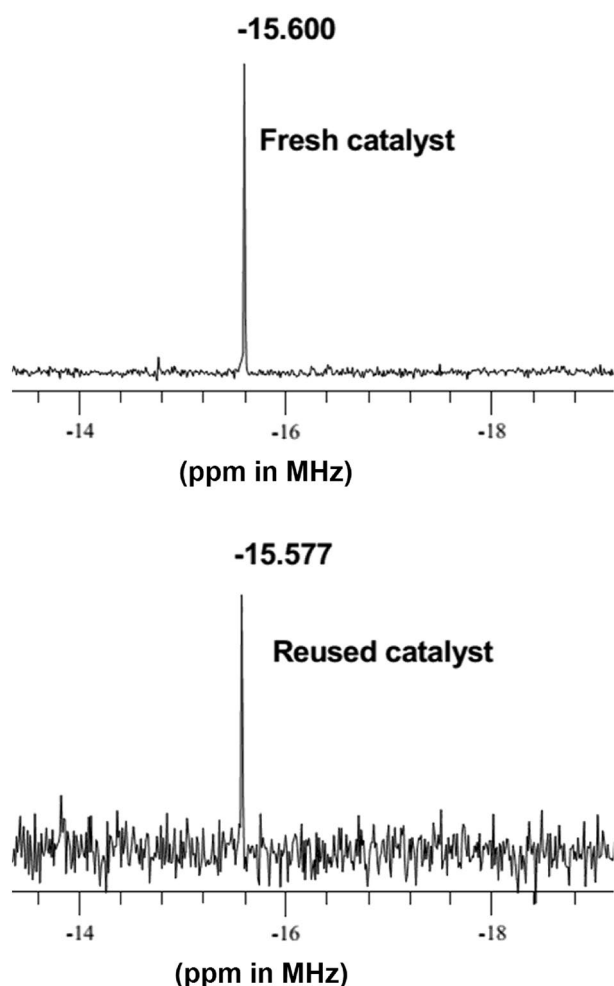


Fig. 9 ^{31}P NMR spectrum of 1-butyl-3-methyl imidazolium phosphotungstate catalyst

peaks of $[\text{BmIM}]^+$ and $[\text{PW}_{12}\text{O}_{40}]^{3-}$ are intact after the fourth run indicating the stability of the catalyst, there is a slight decrease in the intensity of the catalyst recovered after three cycles. This indicates that some amount of catalyst is lost during the reusability cycles.

The stability of Keggin anion before and after four runs was also checked by ^{31}P NMR spectrum in Fig. 9, which revealed no change in the chemical shift value of the reused catalyst when compared with the fresh catalyst. The robustness of the catalyst is low after four catalytic runs as indicated by FTIR and ^{31}P NMR.

4 Conclusion

In conclusion, we propose a simple method for the synthesis of nitrobenzene selectively using smaller amounts of 1-butyl-3-methyl imidazolium phosphotungstate as a

catalyst. The use of *m*-CPBA oxidant produced nitrobenzene with high selectivity when compared to hydrogen peroxide and TBHP. The substituted anilines, irrespective of the electron donating or withdrawing groups present and their positions (ortho, meta and para), also produced the corresponding nitrobenzenes with high selectivities. The catalyst can be recovered easily and reused thrice without loss of catalytic activity.

Acknowledgements The DST-FIST facilities in IIT Madras have been very helpful to carry out this work. We thank VIT-SIF lab, SAS, Chemistry Division, Vellore, for GC-MS analysis.

Compliance with Ethical Standards

Conflict of interest The authors declare that there is no conflict of interest.

References

1. Freemantle M (2010) An introduction to ionic liquids. RSC, Cambridge
2. Seddon KR (1997) Ionic liquids for clean technology. *J Chem Technol Biotechnol* 68(4):351–356
3. Zhao D, Wu M, Kou Y, Min E (2002) Ionic liquids: applications in catalysis. *Catal Today* 74(1):157–189
4. Betz D, Altmann P, Cokoja M, Herrmann WA, Kühn FE (2011) Recent advances in oxidation catalysis using ionic liquids as solvents. *Coord Chem Rev* 255(13):1518–1540
5. Li H, Bhadury PS, Song B, Yang S (2012) Immobilized functional ionic liquids: efficient, green, and reusable catalysts. *RSC Adv* 2(33):12525–12551
6. Kozhevnikov IV (2012) Catalysts for fine chemical synthesis, volume 2, Catalysis by polyoxometalates, Wiley, Weinheim
7. Misono M (2001) Unique acid catalysis of heteropoly compounds (heteropolyoxometalates) in the solid state. *Chem Commun* 13:1141–1152
8. Zhou Y, Chen G, Long Z, Wang J (2014) Recent advances in polyoxometalate-based heterogeneous catalytic materials for liquid-phase organic transformations. *RSC Adv* 4(79):42092–42113
9. Omwoma S, Gore CT, Ji Y, Hu C, Song YF (2015) Environmentally benign polyoxometalate materials. *Coord Chem Rev* 286:17–29
10. Walsh JJ, Bond AM, Forster RJ, Keyes TE (2016) Hybrid polyoxometalate materials for photo (electro-) chemical applications. *Coord Chem Rev* 306:217–234
11. Ruhlmann L, Schaming D (2015) Trends in polyoxometalates research. Nova, New York
12. Qiao Y, Hou Z (2009) Polyoxometalate-based solid and liquid salts for catalysis. *Curr Org Chem* 13(13):1347–1365
13. Gu Y, Li G (2009) Ionic liquids-based catalysis with solids: state of the art. *Adv Synth Catal* 351(6):817–847
14. Mirzaei M, Eshtiagh-Hosseini H, Alipour M, Frontera A (2014) Recent developments in the crystal engineering of diverse coordination modes (0–12) for Keggin-type polyoxometalates in hybrid inorganic–organic architectures. *Coord Chem Rev* 275:1–8
15. Pathan S, Patel A (2013) Keggin type mono Ni (II)-substituted phosphomolybdate: a sustainable, homogeneous and reusable

- catalyst for Suzuki–Miyaura cross-coupling. *Dalton Trans* 42(32):11600–11606
16. Patel A, Narkhede N, Singh S, Pathan S (2016) Keggin-type lacunary and transition metal substituted polyoxometalates as heterogeneous catalysts: a recent progress. *Catal Rev* 58(3):337–370
 17. Kumar PS, Kumar GD, Baskaran S (2008) Truly catalytic and chemoselective cleavage of benzylidene acetal with phosphomolybdic acid supported on silica gel. *Eur J Org Chem* 36:6063–6067
 18. Rajkumar T, Ranga Rao G (2008) Investigation of hybrid molecular material prepared by ionic liquid and polyoxometalate anion. *J Chem Sci* 120(6):587–594
 19. Rao GR, Rajkumar T, Varghese B (2009) Synthesis and characterization of 1-butyl 3-methyl imidazolium phosphomolybdate molecular salt. *Solid State Sci* 11(1):36–42
 20. Rao GR, Rajkumar T (2008) Investigation of 12-tungstophosphoric acid supported on $Ce_{0.5}Zr_{0.5}O_2$ solid solution. *Catal Lett* 120(3–4):261–273
 21. Leng Y, Wang J, Zhu D, Ren X, Ge H, Shen L (2009) Heteropolyanion-based ionic liquids: reaction-induced self-separation catalysts for esterification. *Angew Chem* 121(1):174–177
 22. Leng Y, Wang J, Zhu D, Shen L, Zhao P, Zhang M (2011) Heteropolyanion-based ionic hybrid solid: a green bulk-type catalyst for hydroxylation of benzene with hydrogen peroxide. *Chem Eng J* 173(2):620–626
 23. Zhu W, Huang W, Li H, Zhang M, Jiang W, Chen G, Han C (2011) Polyoxometalate-based ionic liquids as catalysts for deep desulfurization of fuels. *Fuel Process Technol* 92(10):1842–1848
 24. Leng Y, Wang J, Zhu D, Zhang M, Zhao P, Long Z, Huang J (2011) Polyoxometalate-based amino-functionalized ionic solid catalysts lead to highly efficient heterogeneous epoxidation of alkenes with H_2O_2 . *Green Chem* 13(7):1636–1639
 25. Zhen B, Li H, Jiao Q, Li Y, Wu Q, Zhang Y (2012) SiW₁₂O₄₀-based ionic liquid catalysts: catalytic esterification of oleic acid for biodiesel production. *Ind Eng Chem Res* 51(31):10374–10380
 26. Ramalingam M, Manickam S, Srinivasalu KR, Ismail MB, Deivanayagam E (2016) Ionic immobilization of silicotungstic acid on amine-functionalized zirconia: a mesoporous catalyst for esterification of maleic acid. *Eur J Inorg Chem* 11:1697–1705
 27. Yamaguchi K, Yoshida C, Uchida S, Mizuno N (2005) Peroxotungstate immobilized on ionic liquid-modified silica as a heterogeneous epoxidation catalyst with hydrogen peroxide. *J Am Chem Soc* 127(2):530–531
 28. Selvam T, Ramaswamy AV (1996) A new catalytic method for the selective oxidation of aniline to nitrosobenzene over titanium silicate molecular sieves, TS-1, using H_2O_2 as oxidant. *Chem Commun* 10:1215–1216
 29. Selvam T, Vinod MP, Vijayamohan K (1997) Catalytic and electrocatalytic oxidation of aniline to nitrobenzene over vanadium silicate molecular sieves: VS-1 using t-butyl hydroperoxide (TBHP) as oxidant. *React Kinet Catal Lett* 1(60):137–144
 30. Chang CF, Liu ST (2009) Catalytic oxidation of anilines into azoxybenzenes on mesoporous silicas containing cobalt oxide. *J Mol Catal A* 299(1):121–126
 31. Ratnikov MO, Farkas LE, McLaughlin EC, Chiou G, Choi H, El-Khalafy SH, Doyle MP (2011) Dirhodium-catalyzed phenol and aniline oxidations with T-HYDRO. Substrate scope and mechanism of oxidation. *J Org Chem* 76(8):2585–2593
 32. Sakaue S, Tsubakino T, Nishiyama Y, Ishii Y (1993) Oxidation of aromatic amines with hydrogen peroxide catalyzed by cetylpyridinium heteropolyoxometalates. *J Org Chem* 58(14):3633–3638
 33. Sloboda-Rozner D, Witte P, Alsters PL, Neumann R (2004) Aqueous biphasic oxidation: a water-soluble polyoxometalate catalyst for selective oxidation of various functional groups with hydrogen peroxide. *Adv Synth Catal* 346(2–3):339–345
 34. Ishimoto R, Kamata K, Mizuno N (2012) A highly active protonated tetranuclear peroxotungstate for oxidation with hydrogen peroxide. *Angew Chem Int Ed* 51(19):4662–4665
 35. Firouzabadi H, Amani NI (2001) Tungstophosphoric acid catalyzed oxidation of aromatic amines to nitro compounds with sodium perborate in micellar media. *Green Chem* 3(3):131–132
 36. Bamoharram FF, Heravi MM, Roshani M, Akbarpour M (2006) Catalytic performance of Preyssler heteropolyacid as a green and recyclable catalyst in oxidation of primary aromatic amines. *J Mol Catal A* 255(1):193–198
 37. Owens GS, Abu-Omar MM (2002) Comparative kinetic investigations in ionic liquids using the MTO/peroxide system. *J Mol Catal* 187(2):215–225
 38. Hussain H, Al-Harrasi A, Green IR, Ahmed I, Abbas G, Rehman NU (2014) meta-Chloroperbenzoic acid (m CPBA): a versatile reagent in organic synthesis. *RSC Adv* 4(25):12882–12917
 39. Rocchiccioli-Deltcheff C, Fournier M, Franck R, Thouvenot R (1983) Vibrational investigations of polyoxometalates. 2. Evidence for anion-anion interactions in molybdenum (VI) and tungsten (VI) compounds related to the Keggin structure. *Inorg Chem* 22(2):207–216
 40. Zhao P, Zhang M, Wu Y, Wang J (2012) Heterogeneous selective oxidation of sulfides with H_2O_2 catalyzed by ionic liquid-based polyoxometalate salts. *Ind Eng Chem Res* 51(19):6641–6647
 41. Chen G, Zhou Y, Long Z, Wang X, Li J, Wang J (2014) Mesoporous polyoxometalate-based ionic hybrid as a triphasic catalyst for oxidation of benzyl alcohol with H_2O_2 on water. *ACS Appl Mater Interfaces* 6(6):4438–4446
 42. Crosthwaite JM, Muldoon MJ, Dixon JK, Anderson JL, Brennecke JF (2005) Phase transition and decomposition temperatures, heat capacities and viscosities of pyridinium ionic liquids. *J Chem Thermodyn* 37(6):559–568
 43. Qadir MI, Scholten JD, Dupont J (2015) Ionic liquid effect: selective aniline oxidative coupling to azoxybenzene by TiO_2 . *Catal Sci Technol* 5(3):1459–1462
 44. Liu J, Li J, Ren J, Zeng BB (2014) Oxidation of aromatic amines into nitroarenes with m-CPBA. *Tetrahedron Lett* 55(9):1581–1584
 45. Goyal R, Dumbre D, Konathala LS, Pandey M, Bordoloi A (2015) Oxidative coupling of aniline and desulfurization over nitrogen rich mesoporous carbon. *Catal Sci Technol* 5(7):3632–3638
 46. Venturello C, D'Aloisio R, Bart JC, Ricci M (1985) A new peroxotungsten heteropoly anion with special oxidizing properties: synthesis and structure of tetrahexylammonium tetra (diperoxotungsto) phosphate (3-). *J Mol Catal* 32(1):107–110
 47. McKillop A, Tarbin JA (1987) Functional group oxidation using sodium perborate I. *Tetrahedron* 43(8):1753–1758
 48. McKillop A, Tarbin JA (1983) Sodium perborate—a cheap and effective reagent for the oxidation of anilines and sulphides. *Tetrahedron Lett* 24(14):1505–1508